Numerical investigation of the properties of nonlinear acoustical vortices through weakly heterogeneous media

Régis Marchiano,* François Coulouvrat, and Lili Ganjehi
Institut Jean le Rond d'Alembert (UMR CNRS 7190), Université Pierre et Marie Curie-Paris 6 4, place Jussieu 75252, Paris, Cedex 05, France

Jean-Louis Thomas
Institut des NanoSciences de Paris (UMR CNRS 7588), Université Pierre et Marie Curie-Paris 6 140, rue de Lourmel 75015, Paris, France

(Received 9 October 2007; published 23 January 2008)

Acoustical vortices (AV) are the acoustical equivalent of optical vortices (OV) that are a key feature in the discipline of singular optics. For linear waves, OV and AV possess the same properties. But as nonlinearities are different in optics and acoustics, the nonlinear behavior of these structures has to be different. In this paper, a numerical investigation of the three-dimensional (3D) nonlinear propagation of acoustical vortices through homogeneous or heterogeneous media is reported. First, an original numerical method is described and compared to existing ones. Then, it is used to study the dynamics of AV in a nonlinear regime. The nonlinear properties of acoustical vortices in a homogeneous medium are investigated. It is shown that shock waves can be produced during propagation, leading to an interesting spatiotemporal wave field with an azimuthal shock. The dynamics of the topological charge, intrinsic property of AV or OV, is studied in the nonlinear regime through different focusing lenses. Inversion of the topological charge is observed if the AV propagates through a 1D focusing medium (cylindrical lens), while the charge remains constant if the medium is 2D (spherical lens). These last results already observed in linear optics are generalized here to the nonlinear behavior through the investigation of harmonics which show the same behavior as the fundamental with respect to inversion.

DOI: 10.1103/PhysRevE.77.016605 PACS number(s): 43.25.+y, 03.50.−z, 42.65.−k

I. INTRODUCTION

A wave can be described by its amplitude, its phase, and its polarization. Under some circumstances, one of these quantities can be undetermined. If the phase is undetermined, then the wave possesses a phase singularity. Phase singularities can be classified into three categories: edge, screw, or mixed type dislocations of wave front [1]. Nye and Berry [1] showed how these structures are generic and important for the wave's theory. Since that seminal paper, importance of phase singularities (especially screw dislocations) is increasing in many fields of physics: optics, Bose-Einstein condensates, liquid crystals, etc. The best example is optics for which a field of research called singular optics has risen up [2]. Singular optics deals mainly with the study of optical vortices (OV). Acoustical vortices (AV) are the acoustical equivalent of OV, with phase singularities of the screw type. It means their phase has a helical shape winding up around a line where the phase is not defined (the phase singularity). The number of 2π jumps of the phase appearing along a close contour containing the phase singularity is called the topological charge (denoted l in the paper). The topological charge is an integer which can be positive or negative. Its sign is obtained from the direction of rotation for which the phase has positive jumps. The convention is that the sign is positive if the rotation is counterclockwise and negative if the rotation is clockwise [3]. Figure 1 presents numerical simulation of a single acoustical or optical vortex with a charge +1. This particular shape of the phase induces a particular amplitude pattern. At the location of the phase singularity, the amplitude of the field is null so that there is a "dark" core. If the vortex is embedded in a Gaussian envelope, then the root mean square (RMS) amplitude representation shows that the vortex is characterized by a "bright" ring surrounding a "dark" core. This pattern is also referred in optics as the doughnut shape. If the propagation is linear, AV and OV have the same properties. First of all, there are generic features of the wave field [1]. In optics, OV are naturally produced by laser cavities [4]. In acoustics, Hefner and Marston [5] showed experimentally that only four transducers with $\pi/2$ phase shift are sufficient to produce AV. Also, AV or OV with a unity topological charge are structurally stable [6]. Small perturbations do not destroy the phase pattern (see [7] in optics and [8] in acoustics). Moreover, OV or AV carry an angular momentum [9]. This property can also be interpreted as a conservation law of the topological charge. Thomas and Marchiano [10] showed that if the propagation medium is inviscid and isotropic, then the topological charge is constant during the propagation. This theoretical result is valid both for acoustical waves and electromagnetic waves in dielectric media. It generalizes a previous study valid only for electromagnetic waves in vacuum [9]. The conservation of the topological charge is a good example of interesting properties valid both for acoustics or optics. Nevertheless, if waves are not linear, the physical behavior is different. In this paper, we propose a numerical investigation of the properties of acoustical vortices in nonlinear regime through homogeneous media and also weakly heterogeneous ones. The numerical investigation is made

*marchi@lmm.jussieu.fr

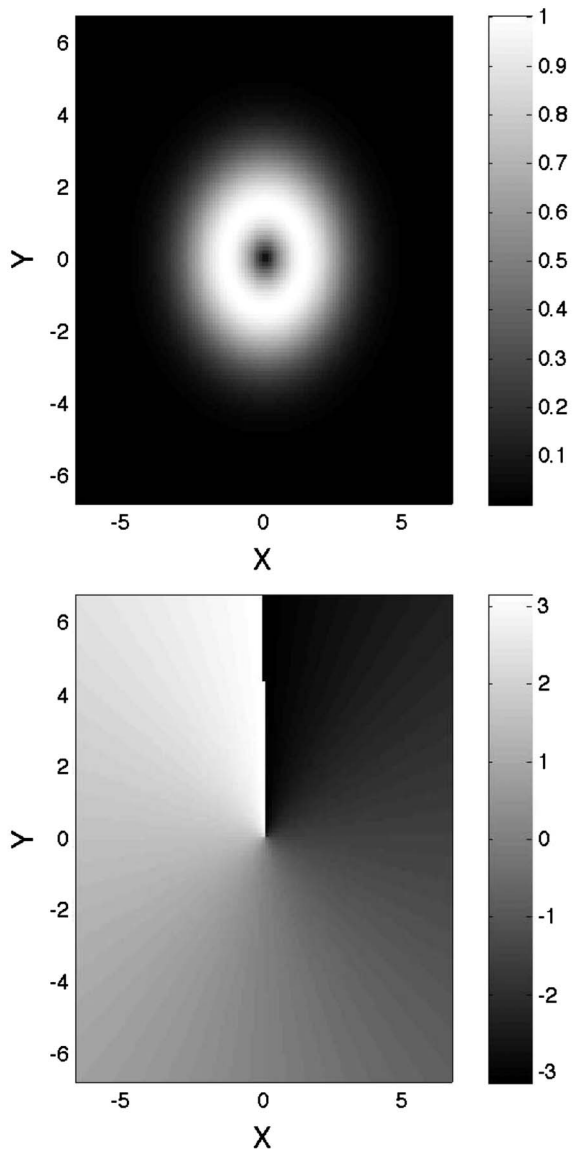

FIG. 1. RMS amplitude (top view) and phase (bottom view) of a single linear vortex of charge 1 in the plane $(X,Y,Z=0)$.

with a code able to handle the three-dimensional (3D) one-way paraxial propagation of nonlinear waves in weakly heterogeneous media. The algorithm is based on a spectral treatment of the diffraction associated with a semianalytical solution of the nonlinear effects. It is an algorithm which is described here. It allows one to explore the complex behavior of AV in the nonlinear regime. Particular attention has been paid to strongly nonlinear vortices with shock waves in homogeneous media, and the propagation of nonlinear AV through 1D or 2D lenses. Section II is devoted to the presentation of the numerical code. Section III deals with the propagation of acoustical vortices in strongly nonlinear regime, especially when shock waves are generated, leading to the formation of an azimuthal shock. Finally, Section IV presents the features of the nonlinear propagation of AV through heterogeneous media.

II. THEORETICAL AND NUMERICAL MODEL

A. Physical model

A particular category of acoustical vortices is the so-called Gauss-Laguerre (GL) beams which are known to carry screw dislocations. Basically (see Sec. III for more details), they are made by an helical phase nested in a Gaussian envelope. For linear propagation, the GL beams are solutions of the paraxial equation [11]. Consequently, the propagation of these structures is well described in the framework of the paraxial approximation. This is valid both for optics and acoustics. If the wave's amplitude is sufficiently high, nonlinear effects cannot be neglected. In optics, the propagation is then well described by the nonlinear Schrödinger equation. In acoustics (in fluids), the main nonlinearities are quadratic and proportional to the instantaneous pressure (and not the envelope). Moreover, acoustical waves, contrarily to optical waves, are nondispersive for usual media (air, water,…). These major differences, briefly described above, drastically change the physical behavior of the nonlinear waves between acoustics and optics. For acoustics, the paraxial approximation of the nonlinear wave equation leads to the so-called Khokhlov-Zabolotskaya (KZ) equation [12]. This equation has been generalized to take into account weak heterogeneities in sound speed [13–15]. Under its dimensionless form, the generalized KZ equation is

$$\frac{\partial^2 P}{\partial Z \partial \tau} = \Delta_\perp P + H_c \frac{\partial^2 P}{\partial \tau^2} + \mu \frac{\partial^2 P^2}{\partial \tau^2}, \tag{1}$$

where P is the dimensionless pressure ($P=p/P_0$ with p the physical pressure and P_0 a characteristic pressure), τ is the dimensionless delayed time [$\tau=\omega_0(t-z/c_0)$ with t the physical time, c_0 the mean speed of sound within the ambient fluid, and ω_0 the characteristic angular frequency], $\Delta_\perp$ the tranverse Laplacian $\Delta_\perp=\partial^2/\partial X^2+\partial^2/\partial Y^2$, with $X=2x/a$ and $Y=2y/a$ the dimensionless transverse coordinates (x and y are the physical transverse coordinates and a is a characteristic dimension of the source), Z is the dimensionless coordinate along the main axis of propagation ($Z=z/L_R$ with z the coordinate along the axis of propagation and $L_R=k_0a^2/2$ the Rayleigh distance with k_0 the characteristic wave number $k_0=\omega_0/c_0$), $\mu=L_R/L_S$ is the ratio between the Rayleigh distance and the shock formation distance for a plane wave, H_c is the heterogeneous coefficient defined by the relation

$$H_c(X,Y,Z) = k_0 L_R \frac{c_h - c_0}{c_h} \tag{2}$$

where $c_h(X,Y,Z)$ is the heterogeneous speed of sound. To establish Eq. (1) the variations of c_h are supposed to be small, $\left|\frac{(c_h-c_0)}{c_h}\right| \ll 1$.

B. Numerical resolution

Numerous papers are devoted to the numerical resolution of the KZ or Khokhlov-Zabolotskaya-Kuznetsov (KZK) equation [16] (that last equation also takes into account the thermoviscous absorption). The main results concern the study of the interaction between diffraction, nonlinearities,

and attenuation during the propagation of a sound beam. Numerical methods can be classified into four categories.

The first one consists in solving the equation entirely in the frequency domain. This method was first applied to calculate the pressure fields produced by axisymmetric sources in the near field [17]. This code is known as Bergen code. It was then used to investigate many other situations: focused beams [18] and interaction between finite amplitude beams [19]. Three-dimensional codes based on this approach have been developed [20–22], most of them were used to investigate the generation of harmonics from a rectangular aperture source. This spectral approach obtained great success. In particular, it is very well adapted to treat attenuation but is not the best method to handle strong nonlinearities such as shock waves accurately. Indeed, because of the spectral treatment of nonlinearities, Gibbs oscillations (artificial oscillations associated to the discrete Fourier transform of a discontinuous signal) appear behind the shocks and so impair the accuracy of the numerical solution.

The last three methods rely on the fractional step procedure [23]. KZK equation is a one-way equation that models propagation along a privileged direction (Z axis). The fractional step procedure consists in separating the physical effects over a small step ΔZ. The equation is solved over each step by solving separately the various equations relative to the physical mechanisms. The coupling between the various effects is obtained by the repetition of the process.

The second method consists in treating diffraction and attenuation in the frequency domain and nonlinear effects in the temporal domain. This method was proposed by Bakhvalov *et al.* [24]. They treated diffraction in frequential domain with an implicit finite differences scheme, and nonlinear effects in temporal domain with a Godunov method. This pseudospectral approach has also been used to treat the problem of focusing of sonic boom on fold caustics [25] though a generalized KZ equation with the heterogeneous term proportional to the distance from the caustic. Three-dimensional codes based on that approach have been recently developed [26]. The frequency domain is well suited to treat the attenuation effects, and the time domain allows a good treatment of shock waves (depending on the chosen method). The treatment of diffraction is quite well done with finite differences but has the major drawback to be dissipative with a standard first-order implicit scheme, or dispersive with a second-order Crank-Nicholson scheme.

In the third method proposed by Lee and Hamilton [27], the KZK equation is directly solved in the time domain. Different finite differences schemes solve the diffraction, the nonlinear and the attenuation subequations of the split-step procedure. This code is known as Texas code. This numerical resolution relies on an appropriate treatment of the diffraction term which is first integrated with respect to time, then is numerically solved by Simpson's rule and an implicit backward finite difference scheme. The resolution of the nonlinear equation is based on Poisson's solution valid if the propagation distance is less than the shock distance. Three-dimensional solvers based on that approach have been recently proposed [28,29]. More recently, Jing and Cleveland proposed a 3D solver extended to take into account inhomogeneities [15]. Coulouvrat and co-workers [30,31] used this approach to study, respectively, the nonlinear Fresnel diffraction and the focusing of shock waves at a caustic cusp. However, instead of using the KZ equation formulated in pressure, they proposed to solve the KZ equation formulated in potential. This formulation is well adapted to the treatment of the shock waves and does not require very small advancement steps. The nonlinear equation is solved in the temporal domain by the Hayes method [32]. This method has many advantages because it is based on an analytical solution of the inviscid Burgers' equation, so that it is fast and accurate. Nevertheless, the resolution of the diffraction part has the same drawbacks (dissipation and/or dispersion) than those of the second class of algorithms.

The last method does not solve the KZK equation directly but handles diffraction, nonlinearity, and attenuation in a phenomenological way. This technique originally proposed by Christopher and Parker [33] relies again on the split-step procedure. They demonstrated that this approach can be used for axisymmetric sources. The diffraction is taken into account by a technique similar to the angular spectrum (resolution of the wave equation) [34] using the discrete Hankel transform. Zemp *et al.* use the angular spectrum method to solve the 3D problem [35]. Tavakholi and co-workers [36,37] used the same phenomenological approach, but entirely in the time domain by solving the Rayleigh integral. Moreover, this last technique has the major drawback to be very time consuming.

We propose, here, a code to simulate nonlinear three-dimensional propagation through a weakly heterogeneous media. It is based on a pseudospectral approach (similar to the second category of codes described above). Diffraction and heterogeneities are treated by spectral methods (not finite differences) and nonlinear effects are taken into account using Hayes analytical solution. This choice has been done to combine the main advantages of each technique. It allows us to have a code handling diffraction without dissipation or dispersion, and able to capture strong nonlinearities such as shock waves.

The generalized KZ equation (1) can be formulated in terms of the acoustical potential Φ (related to the pressure by the following relation: $P=\frac{\partial\Phi}{\partial\tau}$.):

$$\frac{\partial^2\Phi}{\partial Z\partial\tau}=\Delta_\perp\Phi+H_c\frac{\partial^2\Phi}{\partial\tau^2}+\mu\frac{\partial}{\partial\tau}\left(\frac{\partial\Phi}{\partial\tau}\right)^2. \tag{3}$$

This formulation is well suited for the numerical resolution of problem with strong nonlinearities. It corresponds to a weak formulation of the problem where the discontinuities (shock waves) are replaced by angular points. The classical split-step procedure is used to handle separately diffraction, heterogeneities, and nonlinear effects. Starting from the pressure at plane $Z=0$, the pressure field is calculated plane by plane, all planes being parallel. Planes are regularly spaced with a step ΔZ. Calculations between two planes are achieved by the following algorithm:

(1) Calculation of the potential field in the frequency domain by using the Fourier transform with respect to time (denoted $\mathcal{F}_\tau$).

(2) Resolution of the diffraction part of Eq. (3) (left-hand side and the first term of the right-hand side).

(3) Resolution of the heterogeneity part of Eq. (3) (left-hand side and the second term of the right-hand side).

(4) Calculation of potential field in the temporal domain by using the inverse Fourier transform (denoted $\mathcal{F}_\tau^{-1}$).

(5) Resolution of the nonlinear part of Eq. (3) (left-hand side and the third term of the right-hand side).

Steps 1 to 5 are repeated for each plane until the final plane is reached. Diffraction and heterogeneity equations are solved in frequency domain. The Fourier transform of the potential is $\hat{\Phi}(X,Y,Z,\omega)=\mathcal{F}_\tau\{\Phi(X,Y,Z,\tau)\}$, with ω the dimensionless angular frequency. Thus the diffraction equation is reduced to

$$-i\omega\frac{\partial\hat{\Phi}}{\partial Z}=\Delta_\perp\hat{\Phi}. \tag{4}$$

This equation can be solved by a method inspired from the angular spectrum method. Introducing the 2D Fourier transform operator in regards to spatial coordinates X and Y, $\mathcal{F}_{(X,Y)}$, the Fourier transform in time and space of the pressure is noted, $\bar{\hat{\Phi}}(k_X,k_Y,Z,\omega)=\mathcal{F}_{(X,Y)}\{\hat{\Phi}(X,Y,Z,\omega)\}$, k_X and k_Y being the conjugate variables of X and Y through the 2D spatial Fourier transform. Applying the 2D spatial Fourier transform operator to the equation of diffraction [Eq. (4)] expressed in the frequency domain allows us to formulate the diffraction problem by a simple ordinary differential equation

$$\frac{\partial\bar{\hat{\Phi}}}{\partial Z}=-i\frac{k_x^2+k_y^2}{\omega}\bar{\hat{\Phi}}. \tag{5}$$

The solution of this equation is

$$\bar{\hat{\Phi}}(k_X,k_Y,Z,\omega)=\bar{\hat{\Phi}}(k_X,k_Y,Z=0,\omega)\exp\left(-i\frac{k_x^2+k_y^2}{\omega}Z\right). \tag{6}$$

The solution in the (X,Y,Z,ω) space can be calculated by applying the inverse spatial Fourier transform operator to the solution [Eq. (7)],

$$\hat{\Phi}(X,Y,Z,\omega)=\mathcal{F}_{(X,Y)}^{-1}\{\bar{\hat{\Phi}}(k_X,k_Y,Z,\omega)\}. \tag{7}$$

The resolution of the diffraction equation is thus quasiexact since it is based on an analytical solution in the (k_X,k_Y,Z,ω) space.

The heterogeneity equation in the frequency domain is

$$\frac{\partial\hat{\Phi}}{\partial Z}=-i\omega H_c(X,Y,Z)\hat{\Phi}. \tag{8}$$

This equation has to be solved over a ΔZ step. Assuming that the medium is almost homogeneous over ΔZ (which is true if the step ΔZ is sufficiently small), the function H_c depends only on the transverse variables X and Y, so that it is possible to obtain a simple solution of the heterogeneity equation,

$$\hat{\Phi}(X,Y,\Delta Z,\omega)=\hat{\Phi}(X,Y,Z=0,\omega)\exp[-i\omega H_c(X,Y)\Delta Z]. \tag{9}$$

The nonlinear effects are taken into account in the time domain by solving the inviscid Burgers' equation formulated in potential,

$$\frac{\partial\Phi}{\partial Z}=\mu\frac{\partial}{\partial\tau}\left(\frac{\partial\Phi}{\partial\tau}\right)^2. \tag{10}$$

This equation is solved by the Hayes' method [32,30]. This resolution is achieved thanks to an analytical implicit solution of the Burgers' equation (Poisson's solution) taking into account the weak shock theory (the single valued and physically admissible potential is the maximum value of the multivalued ones).

To solve the problem numerically, boundary conditions have to be specified. As seen below, the potential in the source plane $Z=0$ is required. The boundary conditions in X and Y (the tranverse coordinates) are chosen to impose a null potential sufficiently far away from the center of the beam [$\Phi(X\rightarrow\pm\infty,Y,Z,\tau)=0$ and $\Phi(X,Y\rightarrow\pm\infty,Z,\tau)=0$].

To summarize, the numerical procedure to solve the generalized KZ equation described below is based on a pseudospectral algorithm. This allows us to treat the diffraction and heterogeneity without numerical dispersion and/or dissipation in a fast way thanks to the fast Fourier transform (FFT) algorithms. Note that, absorption and/or dispersion can also easily be implemented. Moreover, nonlinearities are efficiently taken into account in the time domain by the Hayes' method. This allows one to deal with strong nonlinear effects such as shock waves (see Sec. III). All the calculations are performed on the potential variable. The pressure is computed only in the last plane by a numerical derivation of the potential, achieved by a standard centered second-order finite differences scheme. The numerical procedure is applied in the next sections to investigate properties of acoustical vortices. Of course, acoustical vortices are not the only physical objects which can be studied by this numerical tool and the algorithm is adapted to many various other situations.

III. NONLINEAR PROPAGATION OF ACOUSTICAL VORTICES THROUGH HOMOGENEOUS MEDIA

The Gauss-Laguerre (GL) beams are known to carry a screw dislocation and can be qualified as "acoustical vortices." They have the double advantage to have a limited spatial extension (and consequently to be of finite energy), and to be a solution of the paraxial equation in linear regime [11]. The pressure associated to a GL beam at point (R,ϕ) [(R,ϕ) are the dimensionless cylindrical coordinates with R the dimensionless radial coordinate defined by $R=(2/a)\sqrt{x^2+y^2}$, and ϕ the angle locating the current point in the transverse plane] in a plane parallel to the source plane and located at a distance Z from it, can be expressed by the following dimensionless formulation [11]:

$$P(R,\phi,Z,\tau)=P_{n,l}(R,\phi,Z)\exp(-i\tau), \tag{11}$$

where the dimensionless variables are defined in Sec. II A and the term $P_{n,l}(R,\phi,Z)$ describes the pressure distribution in the planes transverse to the direction of propagation,

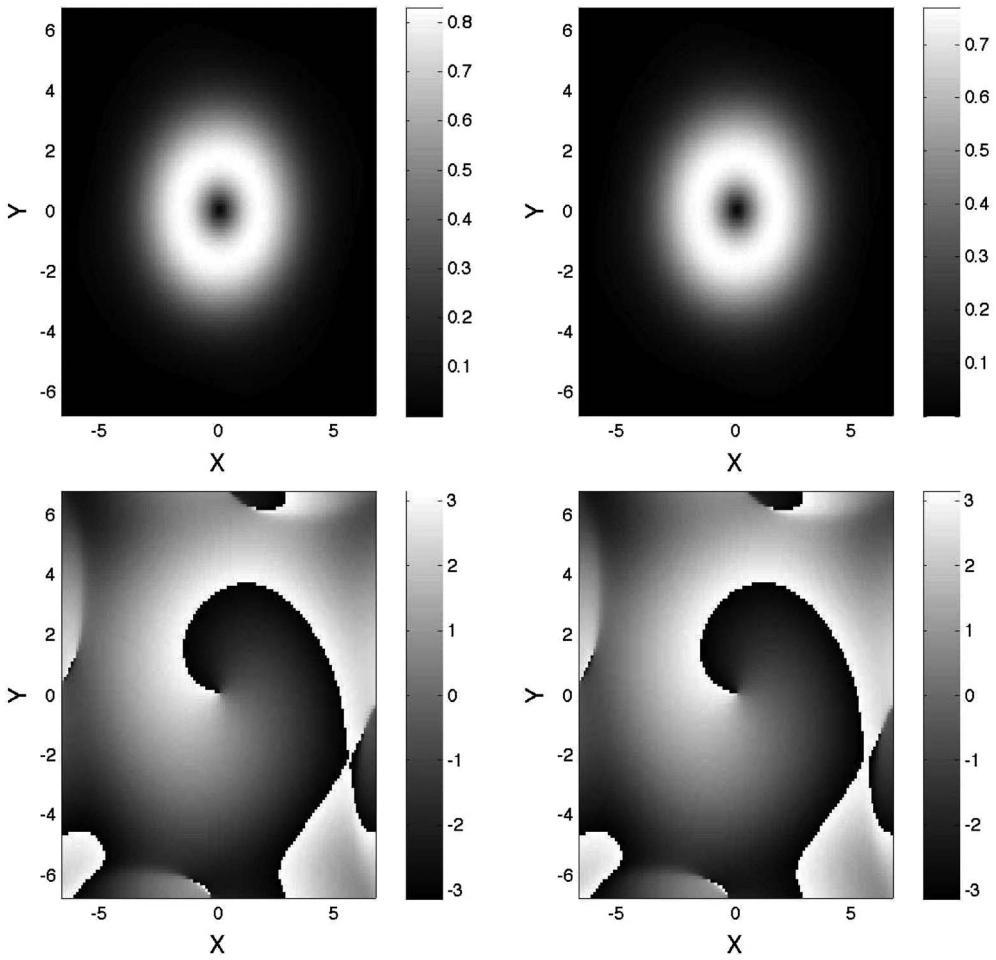

FIG. 2. RMS amplitude (top view) and phase (bottom view) of the pressure field at the fundamental frequency in the plane $Z=0.6$ for a linear ($\mu=0$, left column) and a nonlinear ($\mu=1.53$, right column) AV.

$$P_{n,l}(R,\phi,Z) = G(R,Z)A_{n,l}(R,Z)\Phi_l(\phi)\Psi_n(Z). \quad (12)$$

The different terms in that last expression, respectively, describe the Gaussian envelope of the beam (G), the amplitude structure near the dark core ($A_{n,l}$), the phase structure of the beam Φ_l, and the Gouy phase Ψ_n.

The Gaussian envelope of the beam is

$$G(R,Z) = \frac{D}{(1+Z^2)^{1/2}} \exp\left(\frac{-R^2}{1+Z^2}\right)\exp\left(-i\frac{R^2 Z}{4(1+Z^2)}\right), \quad (13)$$

where D is a normalization constant.

The amplitude structure near the center of the beam is given by

$$A_{n,l}(R,Z) = \left(\frac{R\sqrt{2}}{(1+Z^2)^{1/2}}\right)^{|l|} L^{|l|}_{(n-|l|)/2}\left(\frac{2R^2}{1+Z^2}\right), \quad (14)$$

where $L^{|l|}_{(n-|l|)/2}$ denotes the generalized Laguerre polynomials [38] with $n=|l|,|l|+2,|l|+4,\ldots$. the radial index and l the topological charge.

The helical structure of the phase of the beam is due to the term

$$\Phi_l(\phi) = \exp(il\phi). \quad (15)$$

An additional phase term is required to take into account the Gouy phase,

$$\Psi_n(z) = \exp[-i(n+1)\arctan(Z)]. \quad (16)$$

The linear propagation has been extensively studied. However, as already mentioned, the nonlinear propagation is different in optics and acoustics. In acoustics (in fluids), the classical nonlinearities are quadratic [see Eq. (1)]. They introduce a dependence of the speed of sound proportional to the instantaneous pressure. One consequence is the deformation of the temporal profile of the wave, which can lead to the formation of shock waves. In the frequency domain, the nonlinearities induce a cascade of harmonics of the fundamental frequency (for a continuous wave), all the harmonics being produced by an energy pumping process. Thomas and Marchiano [10] showed theoretically and experimentally that the ratio between the topological charge and the frequency has to be constant for propagation in an inviscid and isotropic medium. Hence, the p harmonic of the fundamental will display a topological charge pq, if the charge of the fundamental is q. This law is valid both for acoustics and optics and is in agreement with the experimental observations. It

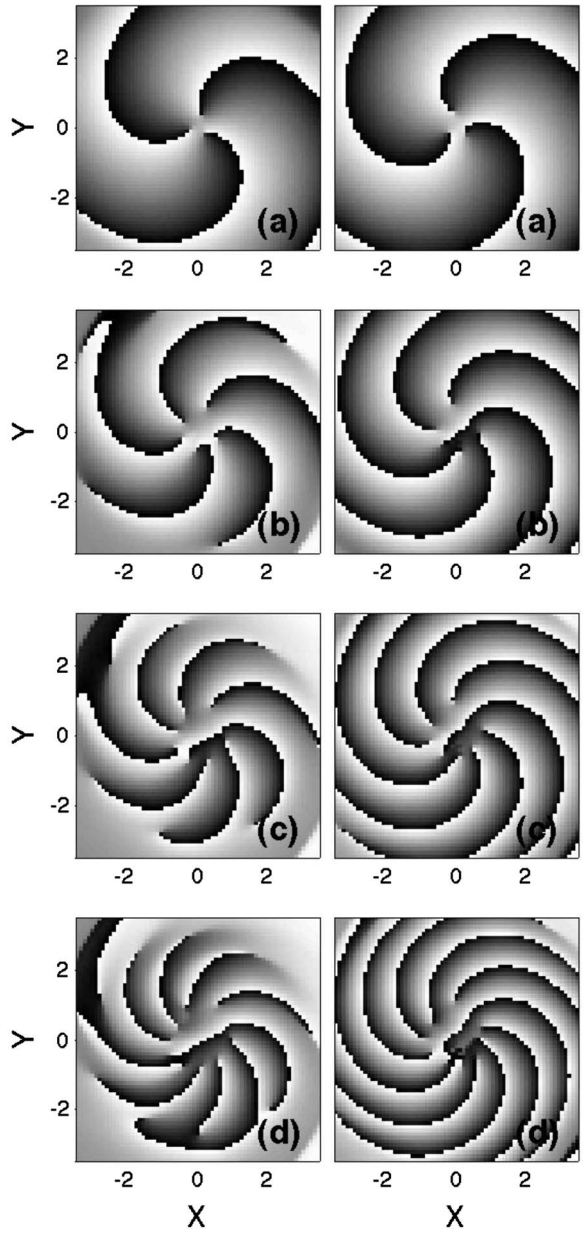

FIG. 3. Phase for the (a) third, (b) fifth, (c) seventh, and (d) ninth harmonic in planes $(X,Y,Z=0.6)$ (left row) and $(X,Y,Z=1)$ (right row) of a single nonlinear AV ($\mu=1.53$).

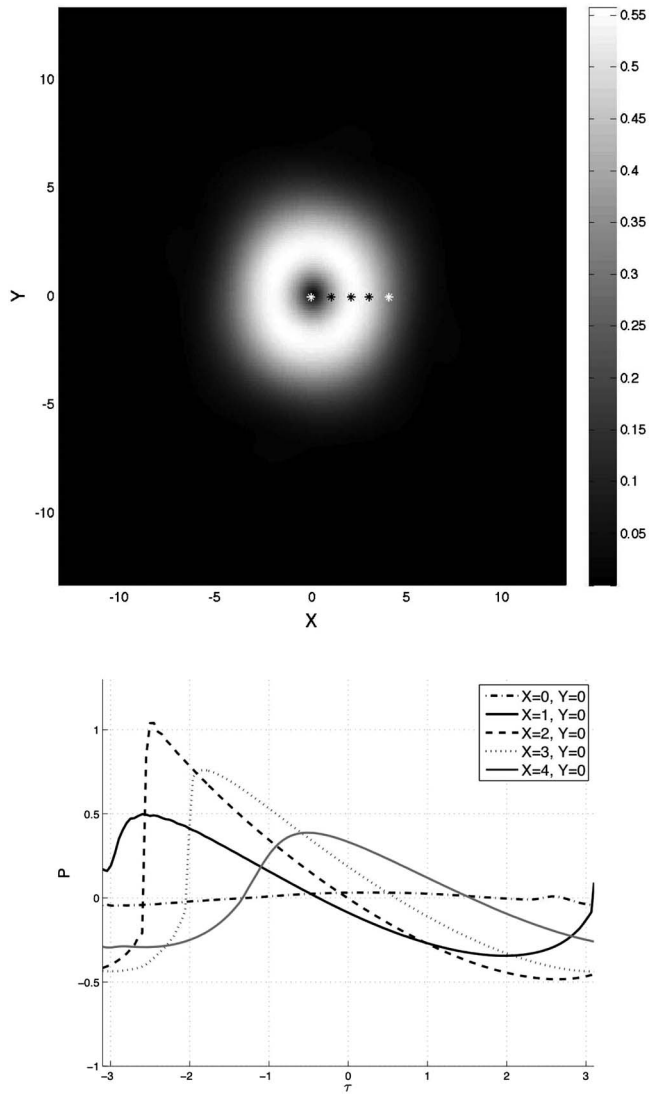

FIG. 4. RMS amplitude in plane $Z=1$ (top view) and pressure versus time at points $(X=0,Y=0)$, $(X=1,Y=0)$, $(X=2,Y=0)$, $(X=3,Y=0)$, and $(X=4,Y=0)$ (bottom view) for a nonlinear AV ($\mu=1.53$). The asterisks in the top view stand for the position of the different points.

was observed in optics [39] that a single OV of charge 1 doubles its charge by passing through a frequency doubling crystal. In acoustics, the generation of harmonics is also accompanied by an increase of the topological charge [10,8]. But in acoustics, contrary to optics, usual media are not dispersive, and the process can be observed on a large number of harmonics.

This law can be checked numerically with the present code. A single vortex of charge one [$l=1$ and $n=1$ in Eq. (11)] is taken at the source ($Z=0$). Its amplitude is chosen sufficiently high to induce nonlinear propagation ($\mu=1.53$, consequently the shock formation distance for a plane wave is $Z=0.65$). Figure 2 shows the RMS amplitude of the pressure and the phase of a linear (left column) and a nonlinear (right column) AV in the plane $Z=0.6$ (less than the shock distance for a plane wave for the nonlinear AV) for the fundamental frequency. As described in the Introduction, the phase clearly displays a helical structure which turns around the center of the beam for which the value of the phase is undefined for both AV. The discontinuity line (jump from white to black) has a spiral shape. This effect is not a nonlinear effect since it is exactly the same for the linear and the nonlinear AV. It is a classical diffraction effect already observed both in optics [3] and acoustics [5]. The RMS amplitude is characterized by a "doughnut" shape. The RMS amplitude and the phase of the fundamental are very similar in linear and nonlinear regime. For the linear regime the amplitude is less than the maximal amplitude of the initial AV (0.8 versus 1), due to the diffraction effects which spread out the energy of the beam on a greater surface than the initial one. For the nonlinear AV, the amplitude is further reduced (0.75

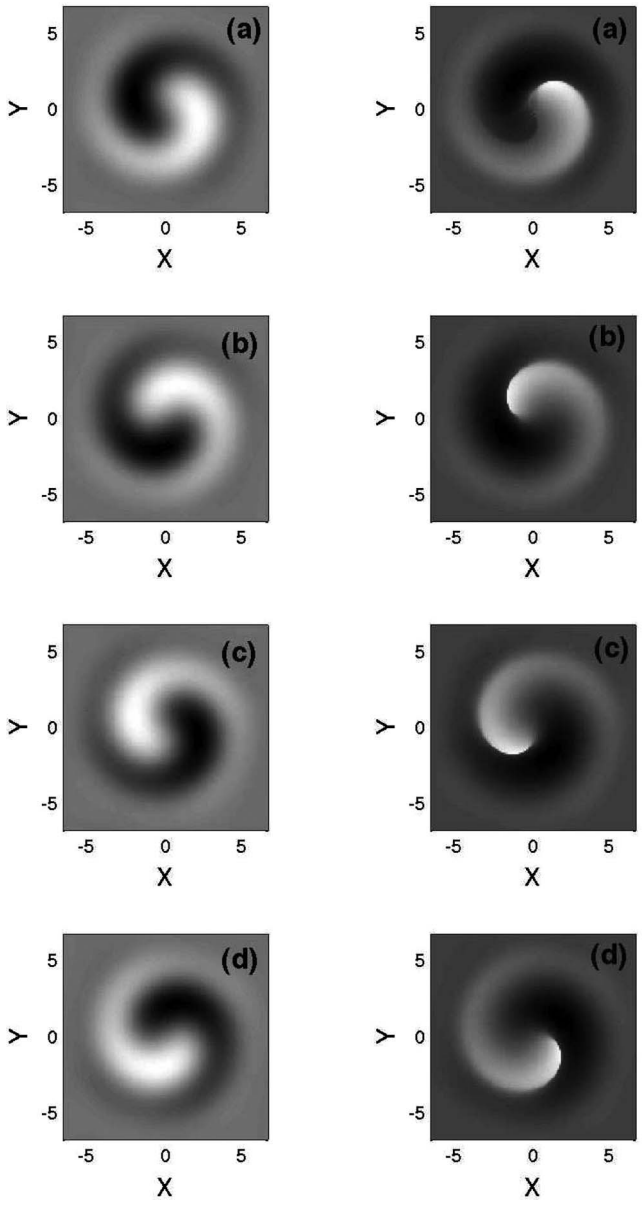

FIG. 5. Instantaneous pressure in the plane $(X,Y,Z=1)$ at four different times: $\tau=0$ (a), $\pi/2$ (b), π (c), and $3\pi/2$ (d), for linear propagation ($\mu=0$, left column) and nonlinear propagation ($\mu=1.53$, right column).

versus 0.8). This is due to the combined effects of diffraction and nonlinearity. Indeed, nonlinear effects induce a transfer of energy from the fundamental frequency to the harmonics.

Figure 3 shows the phase of the beam for the third, fifth, seventh, and ninth harmonics across two parallel planes located in $Z=0.6$ (left column) and $Z=1$ (right view). The first plane corresponds to a propagation distance below the shock formation distance, i.e., in the range of validity of the theoretical law. As expected, the ratio between the total topological charge (visualized by the number of white to black jump when rotating around the center) and the harmonics is constant (equal to one). Nevertheless, it seems that only vortices with unity charge can be produced: for instance when the total charge is 3, this is due to three vortices of charge 1 and not to a single vortex of charge +3. These observations are in

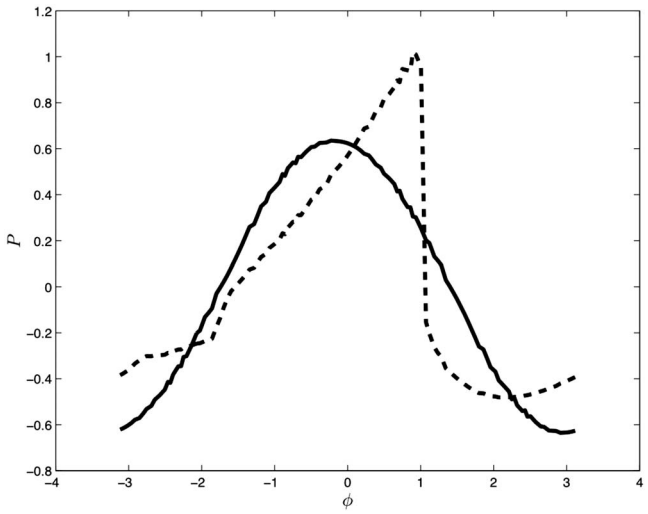

FIG. 6. Dimensionless pressure P versus angle ϕ at radius $R=2$ and at plane $Z=1$ for a linear AV ($\mu=0$, solid line) and a nonlinear AV ($\mu=1.53$, dashed line).

agreement with the concept of structural stability developed by Nye [6] and observed for linear OV [7] and AV [8]. Only vortices with unity charge are stable structures. The smallest perturbations destroy the higher-order vortices which degenerate into unity vortices (nevertheless the *total* topological charge remains constant). The second plane is located beyond the shock formation distance. Rigorously, the conservation law cannot be applied once shocks are formed. Indeed, beyond the shock formation distance, the entropy increases (through pressure jumps) and an energy dissipation occurs through the shocks. Then, the wave propagation cannot be considered as an inviscid process. Nevertheless, these perturbations seems to be weak and gradual enough not to break the conservation law for the total topological charge. No experimental observations have been done for this regime.

Figure 4 shows the RMS pressure (top view) at this distance $(Z=1)$ and the temporal signals (bottom view) for the points $(X=0,Y=0)$, $(X=1,Y=0)$, $(X=2,Y=0)$, $(X=3,Y=0)$, and $(X=4,Y=0)$. The spatial shape of the RMS pressure remains the doughnut, even though the maximal amplitude is decreasing compared to the previous planes (because of energy dissipation and spreading of the beam). At the center of the beam, the pressure is very weak (not exactly zero because of the coupling between nonlinearities and diffraction). At the point $(X=1,Y=0)$ the amplitude is more important. Nonlinear effects take place as shown by the steepening of the wave form. Nevertheless, no shock is visible. At the point $(X=2,Y=0)$ a shock is clearly visible. It is strongly asymmetric, the positive part being much larger than the negative one which is a classical feature of the interaction between diffraction and nonlinearities. At point $(X=3,Y=0)$ a shock wave is still present but its amplitude is weaker than previously observed. Finally, at point $(X=4,Y=0)$, the shock wave is no longer visible as the amplitude of the wave is not sufficient anymore to create a shock wave. This representation of the shock waves is an incomplete view of the situation displaying only the Z-axis projection of the shock (for

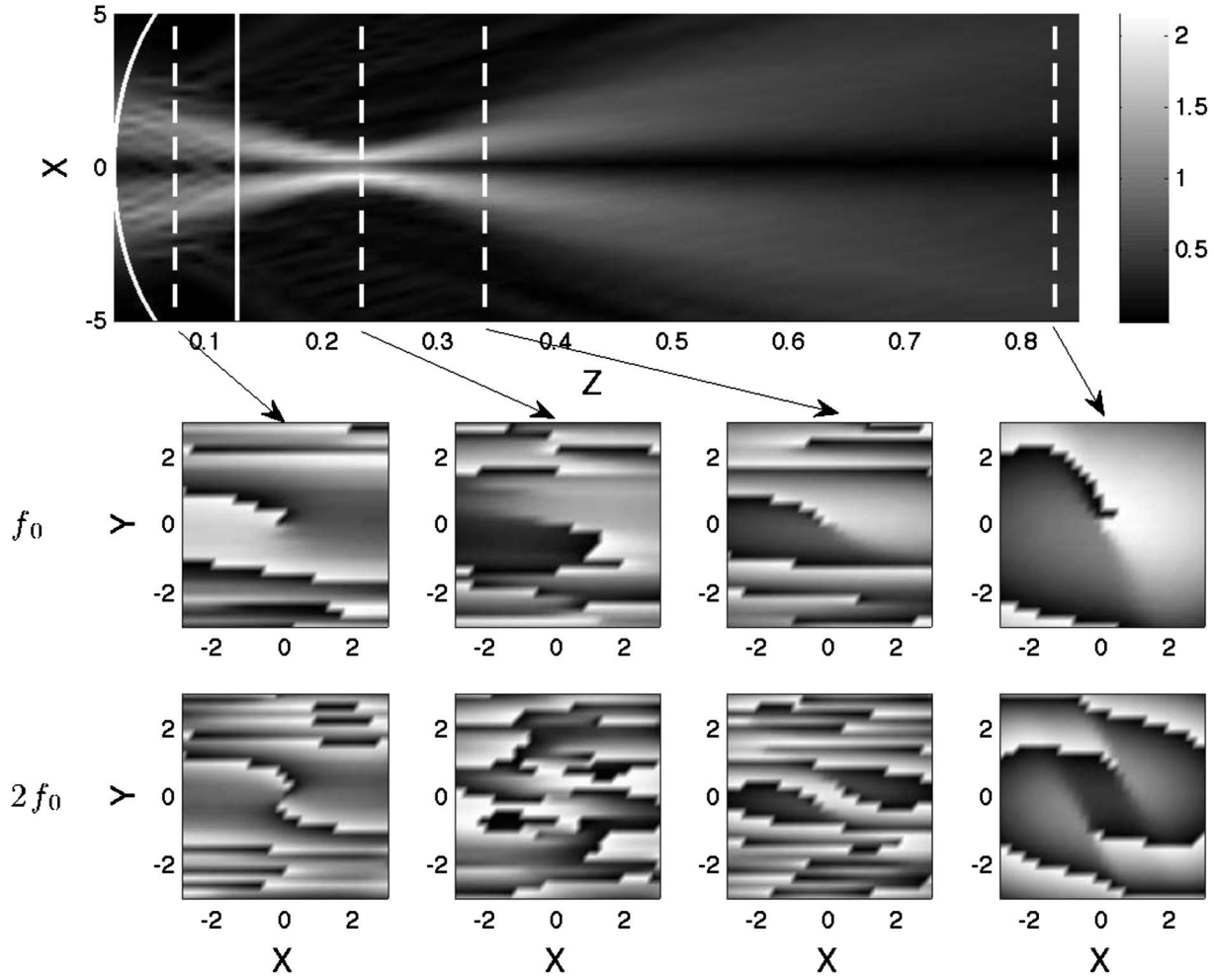

FIG. 7. Nonlinear propagation of a single AV through a 1D acoustical lens. Top view presents the RMS amplitude in the plane (X,Z). Bottom views are representations of the phase for the fundamental frequency and the second harmonic [across plane (X,Y)] at different distances: $Z=0.07$, 0.23, 0.32, and 0.85 (the positions of these planes are indicated by dashed lines on the top view).

paraxial beam, the time dependence is equivalent to the spatial dependence along the Z axis, see definition of the delayed time in Sec. II A). Figure 5 presents the instantaneous pressures over the plane $(X,Y,Z=1)$ at four different times $(\tau=0,\pi/2,\pi,3\pi/2)$ computed for a linear propagation (left column) and a nonlinear propagation with $\mu=1.53$ (right column). This figure shows the spatial distribution of the pressure field. For the linear propagation, there are two lobes (one positive in white and one negative in black). The transition between the two lobes is smooth. A complete rotation of the pattern is achieved in one period. For the nonlinear propagation, the two lobes are still visible. Nevertheless, the transition between them is not smooth everywhere. It exists a small area on each view where a shock wave is visible (sharp transition between white and black). What is visible on this representation is the X and Y components of the shock wave. To clarify this representation, the pressure at a fixed distance R from the center of the beam $(R=2)$ at $T=0$ for all the values of the angle ϕ $(P(R=2,\phi,Z=1,\tau=0))$ is plotted in Fig. 6 for the linear and nonlinear propagation. As expected, the pressure corresponding to the linear case is smooth. But, the pressure computed for the nonlinear propagation presents clearly a shock. This view confirms the conclusions given from Fig. 4, that in the nonlinear regime, there exists an azimuthal shock. It may be of interest for acoustical tweezers since the pressure of radiation is proportional to the spatial derivative of the pressure field for small objects (bubbles, microparticles for instance).

IV. NONLINEAR PROPAGATION OF ACOUSTICAL VORTICES THROUGH HETEROGENEOUS MEDIA

Propagation of AV through a weakly heterogeneous media is now investigated. Two different situations are studied, the first one is the propagation through a 1D acoustical lens and the second one through a 2D acoustical lens. For each case, the source is a single AV with charge +1 and a high amplitude (same AV as in Sec. III). Acoustical lenses are a half cylinder for 1D focusing and a half ball for 2D focusing. To create the focusing effect, the speed of sound of these two lenses is chosen smaller than in the surrounding medium $(c_h/c_0=0.7)$. The axis of the half cylinder is chosen to be the Y axis to create a focusing in the X direction. The half ball creates a focusing in both X and Y directions. The radii of the

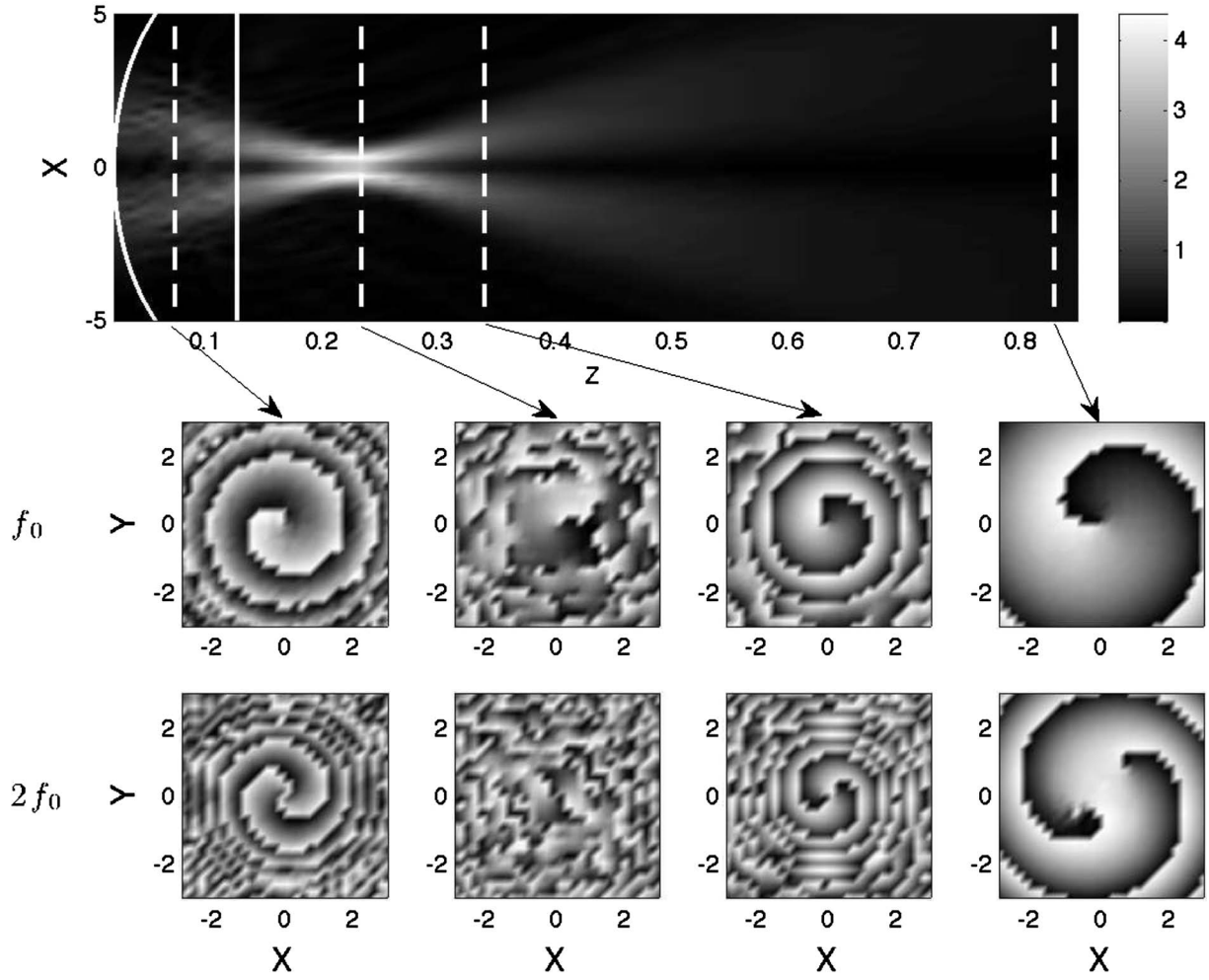

FIG. 8. Nonlinear propagation of a single AV through a 2D acoustical lens. Top view presents the RMS amplitude in the plane (X,Z). Bottom views are representations of the phase for the fundamental frequency and the second harmonic [across plane (X,Y)] at different distances: Z=0.07, 0.23, 0.32, and 0.85 (the positions of these planes are indicated by dash lines on the top view).

half cylinder and the half ball are the same (R_{lenses}=33λ) and these inclusions are located at the same position. The lenses are represented on the top views of Fig. 7 and Fig. 8 by white solid lines. The elliptic shape is due to the fact that the scaling is not the same on the X axis and on the Z axis. Focusing on the X direction is visible on the top views of Figs. 7 and 8. Due to the focusing effect, the acoustical energy is spatially concentrated, and results in an increase of the pressure amplitude. For the 1D focusing the amplification factor is 2 and for the more efficient 2D focusing, the amplification factor is 4. According to the geometries of the lenses, these values were expected. An interesting point is that the zero amplitude along the core of the vortex is present during the whole propagation, even at the focal point (located in Z =0.23).

Figure 7 also presents the evolution of the phase for the 1D lens during the propagation (in four planes located at Z =0.07, 0.23, 0.32, and 0.85) for the fundamental (f_0, first line) and the second harmonic ($2f_0$, second line). Before the focal point, the topological charge is +1 on f_0 and +2 on $2f_0$. The invariance of the ratio between the order of the harmonic and the topological charge explains this result. At the focal point, the pattern exhibits a +1 charge on f_0 and is very noisy on $2f_0$. Hence, this ratio is no longer constant. Beyond the focal point (the last figures), a −1 charge is now visible on f_0 and a −2 charge appears on $2f_0$. Note that the −2 charge is made of two charges −1 and not of a single vortex of charge −2. Again this is related to the concept of structural stability. These results show an inversion of the topological charge of the fundamental and the harmonics. Such an inversion, however restricted to the linear case, has already been observed for OV in an analogous situation (focusing through a cylinder lens) [40]. In practice, the propagation of vortices through cylindrical lenses is important. In optics, this configuration, called cylindrical lens converter, can be used to produced GL beams from Hermite-Gaussian modes [41]. The observations presented here are not in contradiction with the theoretical law of charge conservation. Indeed, in the case of the half cylinder, the isotropy of the medium is broken. Consequently, the law is no longer valid. For a 2D focusing, the situation have to be different as the 2D spherical lens keeps the medium isotropic.

Figure 8 shows the evolution of the phase for the 2D lens during the propagation (in Z=0.07, 0.23, 0.32, and 0.85) for the fundamental (f_0, first line) and the second harmonic ($2f_0$,

second line). Before the focal point, the topological charge is +1 on f_0 and +2 on $2f_0$ in agreement with the theoretical law. For both figures, the discontinuity line on the phase is a spiral which turns in the anticlockwise direction. At the focal point, the topological charge is +1 on f_0, +2 on $2f_0$. The discontinuity lines are now straight lines. Beyond the focal spot, the topological charge is +1 on f_0 and +2 on $2f_0$. There is no inversion of the topological charge in this case. The total topological charge is constant during the whole propagation. Again, that conservation of the topological charge for each harmonic is in full agreement with the conservation law of the topological charge in an isotropic medium. The evolution of the lines of discontinuities is interesting too. Beyond the focal point, the spiral shape is recovered. Nevertheless, the curvature of the spiral arms is now oriented as for a divergent beam and looks similar to a clockwise rotation (see Fig. 2). It shows that diffraction acts as a defocusing effect on the vortex beyond the focal plane. Note that the inversion of the curvature of the spiral arms is not an inversion of the topological charge.

V. CONCLUSIONS AND OUTLOOKS

A numerical tool which allows one to solve numerically the nonlinear paraxial wave equation in a heterogeneous medium has been presented. The treatment of the diffraction and heterogeneities by spectral methods, and the treatment of the nonlinearities by a time domain quasianalytical solution, permits one to obtain fast calculation (the computation time is about 3 hours for $(N_X \times N_Y \times N_Z \times N_T) = (256 \times 256 \times 100 \times 128)$ on a classic PC (xeon 1.8 GHz). This numerical tool is particularly well suited to study the propagation of GL beams because they are the solution of the paraxial equation in linear regime. Numerical investigations show that it is possible to form shock waves inside an acoustical vortex. These shock waves have a tridimensional spiral shape. These results allow us to predict the existence of an azimuthal shock wave associated to nonlinear AV. This original result could be applied to design acoustical devices such as acoustical tweezers. These numerical predictions must be checked experimentally. The results obtained about the focusing through 1D or 2D acoustical lenses outline interesting properties. Depending on the geometry of the acoustical lens, the topological charge can be reversed or not, for the fundamental frequency and all the harmonics. This means that the topological charge contains information on the media and could be used as an information vector to explore mechanical properties of medium. Moreover, the stability of the topological charge (even if it can be inversed for a shock wave) is remarkable, as demonstrated by the zero amplitude stability of the core of a vortex during the propagation through the various acoustical lenses. Again, we think different applications of this property are possible and appealing.

[1] J. F. Nye and M. V. Berry, Proc. R. Soc. London, Ser. A **336**, 165 (1974).
[2] M. S. Soskin and M. V. Vasnetsov, Prog. Opt. **42**, 221 (2001).
[3] M. Mansuripur and E. M. Wright, Opt. Photonics News **1**, 40 (1999).
[4] J. H. Vaughan and D. V. Whillets, J. Opt. Soc. Am. **73**, 1018 (1983).
[5] B. T. Hefner and P. L. Marston, J. Acoust. Soc. Am. **106**, 3313 (1999).
[6] J. F. Nye, *Natural Focusing and Fine Structure of Light* (Institute of Physics Publishing, London, 1999).
[7] V. Y. Bazhenov, M. S. Soskin, and M. V. Vasnetsov, J. Mod. Opt. **39**, 985 (1992).
[8] R. Marchiano and J. L. Thomas, Phys. Rev. E **71**, 066616 (2005).
[9] L. Allen, M. W. Beijersbergen, R. J. C. Spreeuw, and J. P. Woerdman, Phys. Rev. A **45**, 8185 (1992).
[10] J.-L. Thomas and R. Marchiano, Phys. Rev. Lett. **91**, 244302 (2003).
[11] R. Piestun, Y. Y. Schechner, and J. Shamir, J. Opt. Soc. Am. A **17**, 294 (2000).
[12] E. A. Zabolotskaya and R. V. Khokhlov, Sov. Phys. Acoust. **15**, 35 (1969).
[13] P. Blanc-Benon, P. Lipkens, L. Dallois, M. F. Hamilton, and D. T. Blackstock, J. Acoust. Soc. Am. **111**, 487 (2002).
[14] L. Ganjehi, R. Marchiano, F. Coulouvrat, and J. L. Thomas, J. Acoust. Soc. Am. (to be published).
[15] Y. Jing and R. O. Cleveland, J. Acoust. Soc. Am. **122**, 1352 (2007).
[16] V. P. Kuznetsov, Sov. Phys. Acoust. **16**, 467 (1970).
[17] S. I. Aanonsen, T. Barkve, J. N. Tjotta, and S. Tjotta, J. Acoust. Soc. Am. **75**, 749 (1984).
[18] T. S. Hart and M. F. Hamilton, J. Acoust. Soc. Am. **84**, 1488 (1988).
[19] J. N. Tjotta, S. Tjotta, and E. H. Vefring, J. Acoust. Soc. Am. **89**, 1017 (1991).
[20] T. Kamakura, M. Tani, and Y. Kumamoto, J. Acoust. Soc. Am. **91**, 3144 (1992).
[21] A. C. Baker, A. N. Berg, A. Sahin, and J. N. Tjotta, J. Acoust. Soc. Am. **97**, 3510 (1995).
[22] M. D. Cahill, J. Acoust. Soc. Am. **104**, 1274 (1998).
[23] W. F. Ames, *Numerical Methods for Partial Differential Equations* (Academic Press, San Diego, 1977).
[24] N. S. Bakhvalov *et al.*, *Nonlinear Theory of Sound Beams* (American Institute of Physics, New York, 1987).
[25] R. Marchiano, J.-L. Thomas, and F. Coulouvrat, Phys. Rev. Lett. **91**, 184301 (2003).
[26] V. A. Khokhlova, A. E. Ponomarev, M. A. Averkiou, and L. A. Crum, Acoust. Phys. **53**, 481 (2006).
[27] Y. S. Lee and M. F. Hamilton, J. Acoust. Soc. Am. **97**, 906 (1995).
[28] A. Bouakaz, E. Closset, and D. Cathignol, IEEE Trans. Ultrason. Ferroelectr. Freq. Control **50**, 730 (2003).
[29] X. Yang and R. O. Cleveland, J. Acoust. Soc. Am. **117**, 113 (2004).
[30] F. Coulouvrat and R. Marchiano, J. Acoust. Soc. Am. **114**,

1749 (2003).
[31] R. Marchiano, F. Coulouvrat, and J. L. Thomas, J. Acoust. Soc. Am. **117**, 566 (2005).
[32] W. D. Hayes, R. C. Haefeli, and H. E. Kulsrud, NASA Tech. Report No. CR-1299, 1969 (unpublished).
[33] T. Christopher and K. Parker, J. Acoust. Soc. Am. **90**, 488 (1991).
[34] J. W. Goodman, *Introduction to Fourier Optics* (McGraw-Hill, New York, 1968).
[35] R. J. Zemp, J. Tavakkoli, and R. S. Cobbold, J. Acoust. Soc. Am. **113**, 139 (2003).
[36] J. Tavakkoli, D. Cathignol, R. Souchon, and O. A. Sapozhnikov, J. Acoust. Soc. Am. **104**, 2061 (1998).
[37] V. A. Khokhlova, R. Souchon, J. Tavakkoli, O. A. Sapozhnikov, and D. Cathignol, J. Acoust. Soc. Am. **110**, 95 (2001).
[38] M. Abramowitz and I. Stegun, *Handbook of Mathematical Functions* (Dover, New-York, 1965).
[39] I. V. Basistiy, V. Y. Bazhenov, M. S. Soskin, and M. V. Vasnetsov, Opt. Commun. **103**, 42 (1993).
[40] G. Molina-Terriza, J. Recolons, J.-P. Torres, L. Torner, and E. M. Wright, Phys. Rev. Lett. **87**, 023902 (2001).
[41] M. W. Beijersbergen, L. Allen, H. V. der Veen, and J. P. Woerdman, Opt. Commun. **96**, 123 (1993).